Electronic Supplementary Material (ESI) for CrystEngComm.

Supplementary information

Phase-controlled synthesis of iron phosphates via phosphation of β-FeOOH nanorods

Ronghe Lin,[a] Amol P. Amrute,[a] Frank Krumeich,[b] Károly Lázár,[c] Roland Hauert,[d] Maxim Yulikov[e] and Javier Pérez-Ramírez*[a]

[a.] *Institute for Chemical and Bioengineering, Department of Chemistry and Applied Biosciences, ETH Zurich, Vladimir-Prelog-Weg 1, CH-8093 Zurich, Switzerland. Email: jpr@chem.ethz.ch*

[b.] *Laboratory of Inorganic Chemistry, Department of Chemistry and Applied Biosciences, ETH Zurich, Vladimir-Prelog-Weg 1, CH-8093 Zurich, Switzerland.*

[c.] *Department of Nuclear Analysis, Center for Energy Research, MTA, Konkoly-Thege M. 29-33, H-1121 Budapest, Hungary.*

[d.] *Empa, Swiss Federal Laboratories for Materials Science and Technology, Überlandstrasse 129, CH-8600 Dübendorf, Switzerland.*

[e.] *Laboratory of Physical Chemistry, Department of Chemistry and Applied Biosciences, ETH Zurich, Vladimir-Prelog-Weg 2, CH-8093 Zurich, Switzerland.*

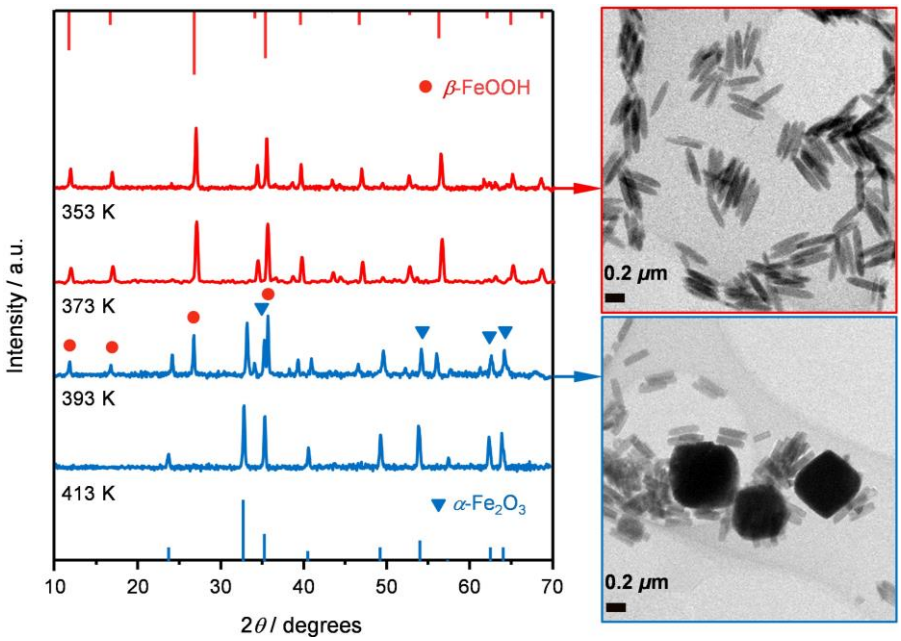

Fig. S1. Synthesis of β-FeOOH nanorods by hydrolysis of $FeCl_3$. X-ray powder diffractograms and corresponding TEM images of the synthesised samples at different hydrothermal temperatures. Vertical lines on the top and bottom axes correspond to the reference β-FeOOH (JCPDS 34-1266) and α-Fe_2O_3 (JCPDS 33-0664), respectively.

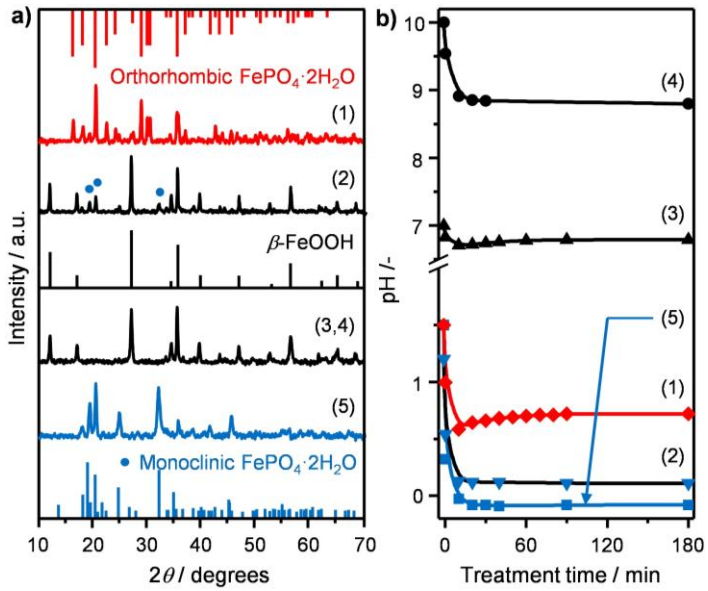

Fig. S2. Influence of pH (1-4) and iron precursor (5) on the formation of $FePO_4{\cdot}2H_2O$ *via* treatment of β-FeOOH-nr (1-4) or $Fe(NO_3)_3$ with H_3PO_4 at P/Fe = 1.8 and 353 K for 3 h (14 h for $Fe(NO_3)_3$ as no precipitate was formed in 3 h). **a**) XRD patterns of the solid samples and **b**) pH evolution as a function of time. (1) pH 1.5 (β-FeOOH/H_3PO_4); (2) pH 1.2 (β-FeOOH/H_3PO_4/HNO_3, this pH value is equal to that of the treatment solution with P/Fe = 8.9); (3) pH 7 (β-FeOOH/H_3PO_4/$NH_3{\cdot}H_2O$); (4) pH 10 (β-FeOOH/H_3PO_4/$NH_3{\cdot}H_2O$); (5) pH 1.5 ($Fe(NO_3)_3$/H_3PO_4), 14 h. Vertical lines in **a**) show the reference orthorhombic (JCPDS 33-667) and monoclinic (JCPDS 33-666) $FePO_4{\cdot}2H_2O$, and β-FeOOH (JCPDS 34-1266).

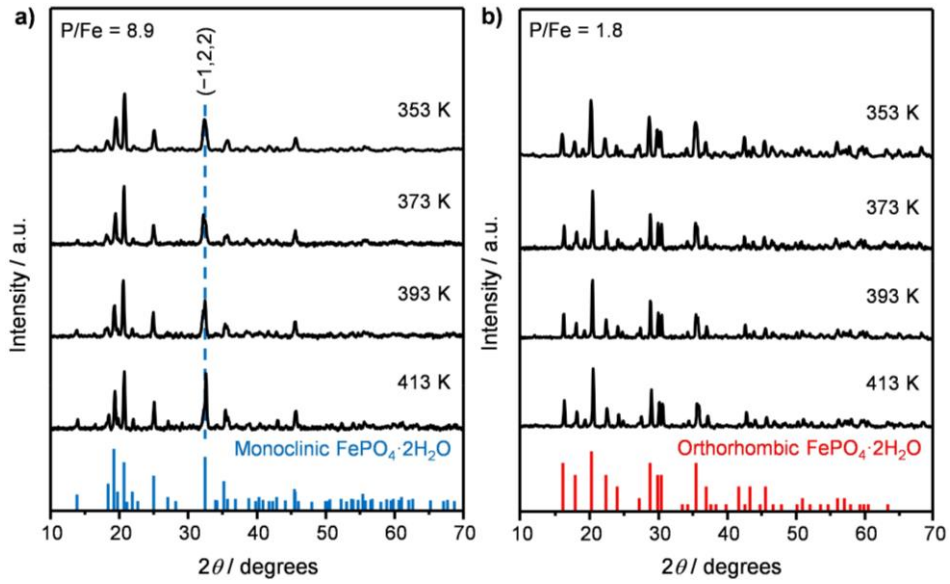

Fig. S3. XRD patterns of samples obtained *via* phosphation of β-FeOOH-nr with H_3PO_4 for 14 h at different temperatures. **a**) P/Fe = 8.9 and **b**) P/Fe = 1.8. Vertical lines on the bottom axes belong to the reference orthorhombic (JCPDS 33-667) and monoclinic (JCPDS 33-666) $FePO_4 \cdot 2H_2O$. The patterns in **a**) indicate the preferential orientation of monoclinic $FePO_4 \cdot 2H_2O$ in the (−1,2,2) direction at $2\theta = 32.17°$ at higher treatment temperatures.

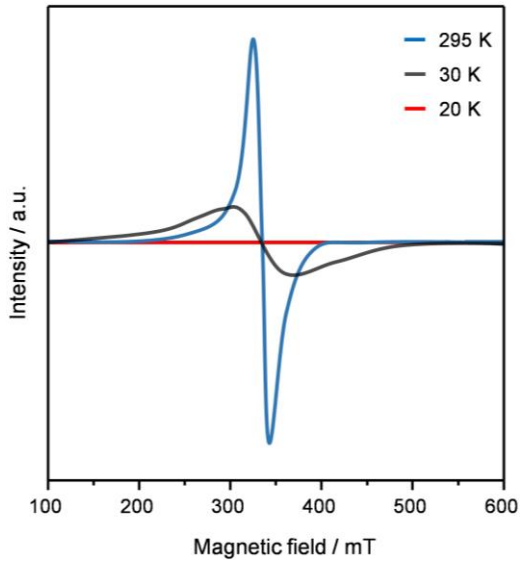

Fig. S4. EPR spectra of $FePO_4$ (derived by calcination of the M-14 sample at 923 K for 5 h) recorded at different temperatures. The EPR line disappears at 20 K, in accordance with the known antiferromagnetic transition of $FePO_4$. Note that the room-temperature spectra were measured with a resonant frequency of 9.886 GHz. The low-temperature spectra were measured with a cryostat tube inserted into the resonator, which shifted the resonance frequency to 9.485 GHz. The room-temperature spectrum was shifted accordingly to adjust the frequency difference. These results confirm that the EPR signals observed in the M-*t* and O-*t* samples are due to the formation of iron phosphates.

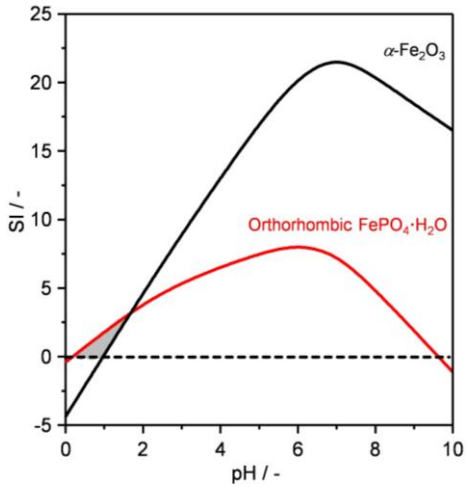

Fig. S5. Saturation index (SI) of orthorhombic $FePO_4 \cdot 2H_2O$ and α-Fe_2O_3 as a function of pH during the phosphation of β-FeOOH-nr with H_3PO_4 at P/Fe = 1.8. The dissolved iron was set as 30 mg Fe g^{-1} β-FeOOH, which was the maximum amount detected by AAS. The influence of other anions on the pH adjustment was not considered. Calculations of SI values were performed using the Visual MINTEQ software. The gray area highlights the narrow pH range in which the formation of orthorhombic $FePO_4 \cdot 2H_2O$ is favorable. The SI of monoclinic $FePO_4 \cdot 2H_2O$ was not calculated due to the unavailability of thermodynamic parameters.

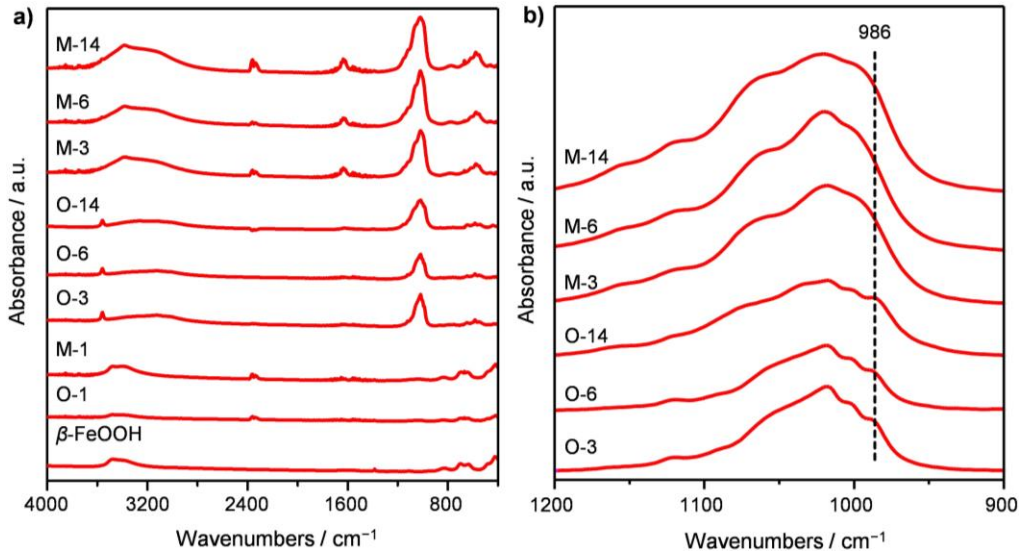

Fig. S6. **a**) FTIR spectra of β-FeOOH-nr and the samples derived from treatment in H_3PO_4. **b**) Enlargement of the range of 900-1200 cm^{-1}, showing the vibrational modes of the phosphate groups in M-*t* and O-*t* samples. Nominal atomic ratios of the M-*t* and O-*t* samples were **a**) P/Fe = 8.9 and **b**) P/Fe = 1.8 respectively, where *t* denotes the treatment time in hours. Among the broad envelop of bands at 950-1100 cm^{-1}, a shoulder at 986 nm^{-1} was observed only for the O-*t* samples. This suggests that at least one extra surface complex was formed during the formation of orthorhombic $FePO_4 \cdot 2H_2O$.

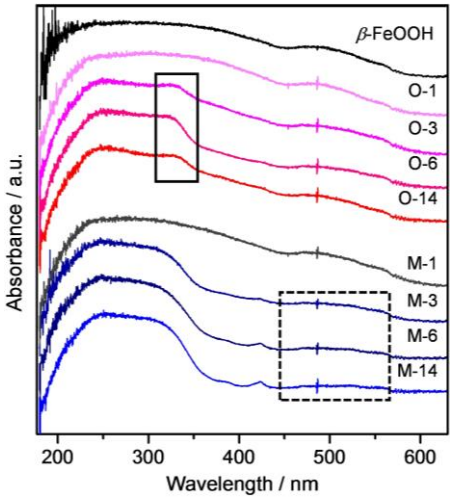

Fig. S7. UV-Vis spectra of β-FeOOH-nr and the samples derived from treatment in H_3PO_4. After 3 h of treatment, the absorption in the visible range virtually disappeared for M-*t* samples as indicated by the dashed box, while a shoulder emerged at *ca.* 320 nm for the O-*t* samples (solid box). These observations further demonstrate that different interactions may occur between β-FeOOH-nr and H_3PO_4 during the formation of different phases of $FePO_4{\cdot}2H_2O$.

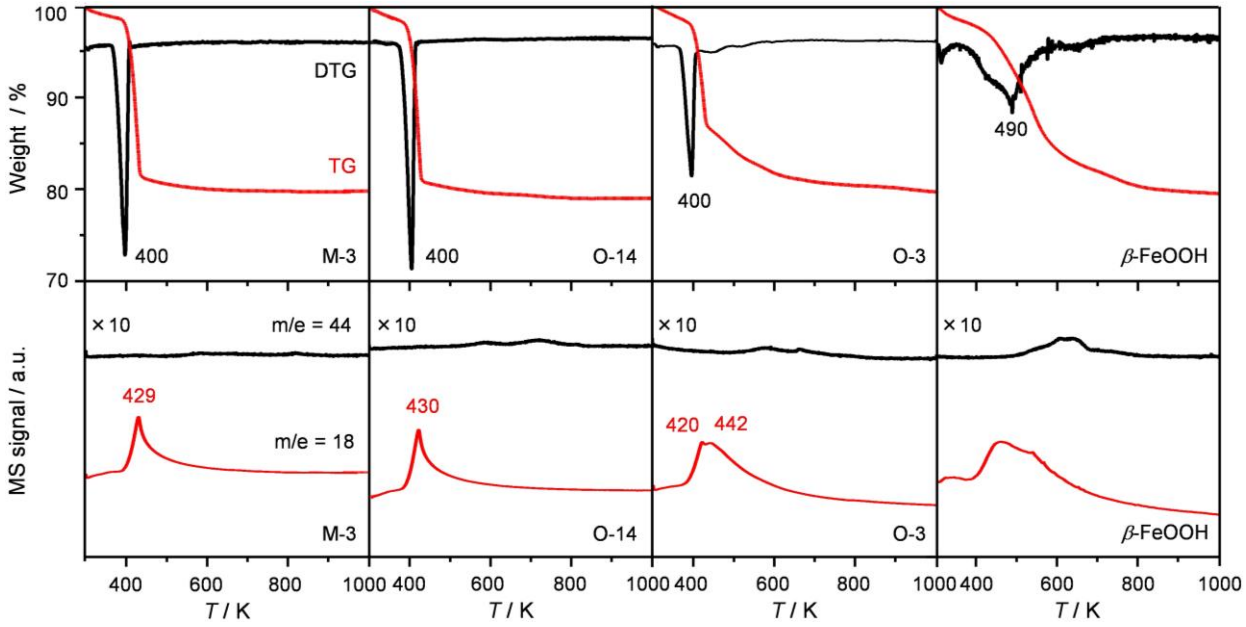

Fig. S8. TGA-MS profiles of monoclinic (M-3) and orthorhombic (O-14) $FePO_4{\cdot}2H_2O$, O-3, and β-FeOOH-nr.

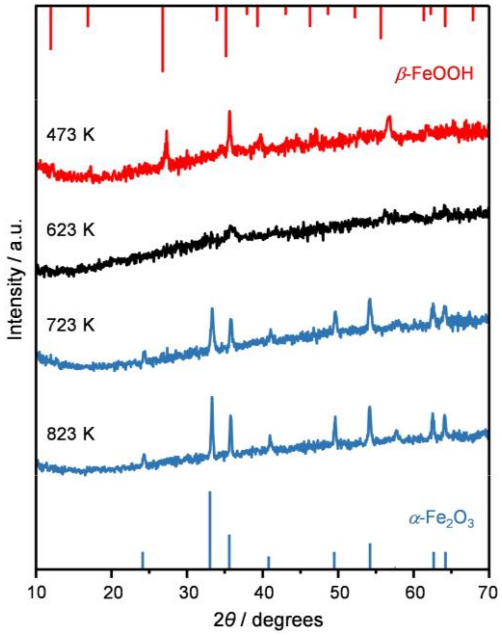

Fig. S9. XRD patterns of β-FeOOH-nr after calcination for 5 h at different temperatures. Vertical lines on the top and bottom axes are the reference β-FeOOH (JCPDS 34-1266) and α-Fe_2O_3 (JCPDS 33-0664).

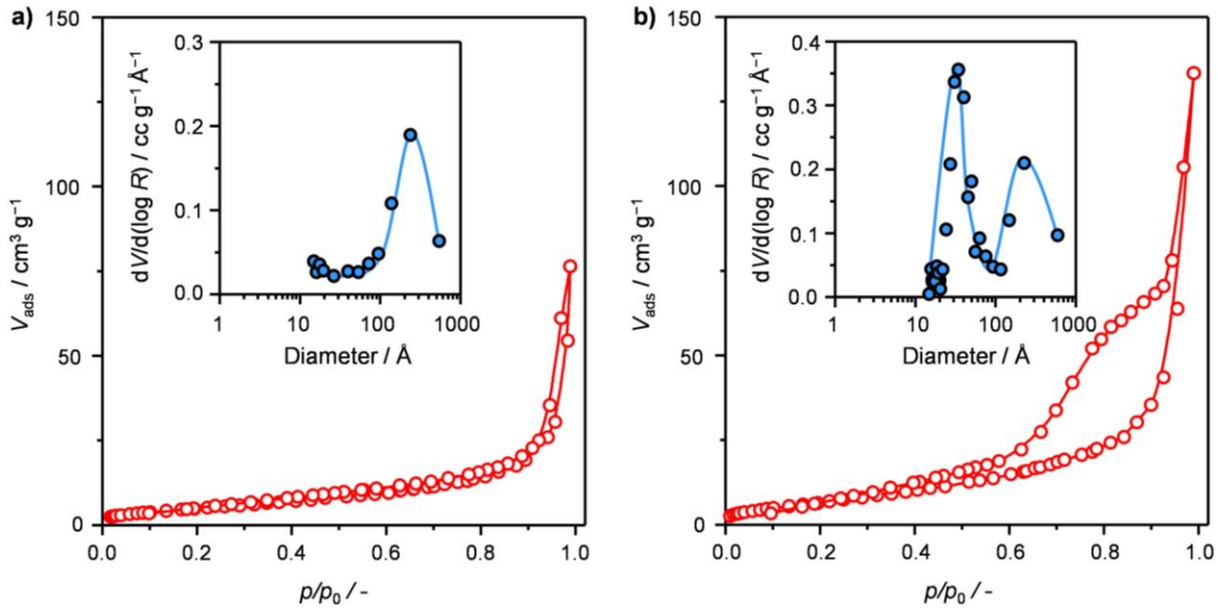

Fig. S10. N_2 sorption isotherms of the **a**) β-FeOOH-nr and **b**) O-3 samples after calcination at 923 K for 5 h. Inset: pore size distribution derived by the BJH method using the desorption branch.